Agricultural and Forest Meteorology 341 (2023) 109677

Contents lists available at ScienceDirect

Agricultural and Forest Meteorology

journal homepage: www.elsevier.com/locate/agrformet

Time-lag effects of flood stimulation on methane emissions in the Dongting Lake floodplain, China

Tao Wang [a,b,c], Zhengmiao Deng [a,b,*], Yonghong Xie [a,b], Buqing Wang [d], Shaoan Wu [d], Feng Li [a,b], Wei Wang [a,b], Yeai Zou [a,b], Xu Li [a,b], Zhiyong Hou [a,b], Jing Zeng [a,b], Mei Wang [e], Changhui Peng [f,g]

[a] Key Laboratory of Agro-Ecological Processes in Subtropical Region, Institute of Subtropical Agriculture, Chinese Academy of Sciences, Changsha 410125, Hunan, China
[b] National Field Scientific Observation and Research Station of Dongting Lake Wetland Ecosystem in Hunan Province, Changsha 410125, Hunan, China
[c] University of Chinese Academy of Sciences, Beijing 100049, China
[d] Changsha General Survey of Natural Resources Center, China Geological Survey, Changsha 410600, China
[e] School of Geographic Sciences, South China Normal University, Guangzhou 510631, China
[f] School of Geographic Sciences, Hunan Normal University, Changsha 410081, China
[g] Department of Biology Sciences, University of Quebec at Montreal, C.P. 8888, Succ. Centre-Ville, Montreal H3C 3P8, Canada

ARTICLE INFO

Keywords:
Floodplain wetlands
Methane emissions
Time-lag effect
Flood stimulation

ABSTRACT

Natural wetlands are the primary sources of CH_4 emissions in the natural environment. However, the understanding of CH_4 fluxes in floodplain wetlands remains limited. This study employed eddy covariance methods to observe CH_4 fluxes over a three-year period in a subtropical wetland floodplain, specifically the *Miscanthus sacchariflorus* (*M. sacchariflorus*) ecosystem in Dongting Lake wetland. Our analysis focused on exploring the impact of flooding frequency on CH_4 emissions, flood stimulation effect, time-lag effects, and the environmental factors influencing CH_4 fluxes. The *M. sacchariflorus* ecosystem exhibited an annual CH_4 emission rate of 14.54 g CH_4—C m^{-2} y^{-1}. During the flood period, the average daily CH_4 emissions reached 0.155 g CH_4—C m^{-2} d^{-1}, contrasting with the pre-flood period's average of 0.014 g CH_4—C m^{-2} d^{-1}. Moreover, the time-lag effect of flooding on CH_4 emissions was found to be 10 days, representing the period between inundation and a substantial increase in CH_4 emissions. Comparatively, in 2021, following three fluctuations in floodwaters, the average CH_4 emission intensity during the flood period decreased by 46.2% and 48.9% when compared to the years 2019 and 2020 which both following one fluctuation, respectively. CH_4 emissions during flooding are predominantly influenced by water depth (WD), wherein shallow WD corresponds to higher CH_4 emissions. This correlation can be attributed to factors such as vegetation type, water-column pressure, and soil oxygen content. Therefore, increasing frequency of inundation and a higher WD hold promise as effective measures for mitigating CH_4 emissions in floodplain wetlands.

1. Introduction

Increasing concentrations of atmospheric CH_4 pose a major global concern. Wetlands have been identified as a prominent natural source of atmospheric CH_4 (Turetsky et al., 2014), accounting for approximately 1/3 of the total global emissions (Dalmagro et al., 2019; Kirschke et al., 2013; Rosentreter et al., 2021). Accurately quantifying CH_4 emission rates and forecasting their environmental effects are of utmost importance in the face of a changing climate, particularly concerning inland wetlands (Kim et al., 2020; Saunois et al., 2016).

Tower-based Eddy Covariance (EC) measurements provide a valuable means of capturing ecosystem-scale CH_4 fluxes with a high temporal resolution. By integrating these measurements with data on key CH_4 drivers such as temperature, water, and different vegetation types, researchers can contribute to CH_4 budget assessments and explore the underlying mechanisms regulating CH_4 environmental dynamics. Although EC towers have been utilized to measure CO_2 fluxes since the late 1970s (Anderson et al., 1984; Desjardins, 1974), it was not until the

* Corresponding author at: Key Laboratory of Agro-Ecological Processes in Subtropical Region, Institute of Subtropical Agriculture, Chinese Academy of Sciences, Changsha 410125, Hunan, China.
E-mail address: dengzm@isa.ac.cn (Z. Deng).

https://doi.org/10.1016/j.agrformet.2023.109677
Received 15 June 2023; Received in revised form 15 August 2023; Accepted 20 August 2023
Available online 24 August 2023
0168-1923/

1990s that some towers began monitoring CH_4 fluxes (Verma et al., 1992). However, most EC measurements focusing on CH_4 fluxes have been conducted within the last decade (the 2010s) (Delwiche et al., 2021). While investigations into CH_4 fluxes and their associated environmental impact factors in high-latitude peatlands have received substantial attention (Huang et al., 2021; Scheller et al., 2021; Zhang et al., 2019), comparatively limited data have been published concerning subtropical and/or tropical regions, which encompass large floodplain areas (Winton et al., 2017). Therefore, there is a significant knowledge gap in understanding CH_4 dynamics and related environmental impacts within these regions. Consequently, continuous monitoring of CH_4 fluxes in floodplain wetlands is essential for improving the global CH_4 flux dataset and elucidating the effects of flooding on CH_4 emissions.

Seasonal floodplains of natural origin are recognized as highly dynamic, diverse, and productive ecosystems worldwide (Batson et al., 2015; Ren, 2020). Among the various factors influencing CH_4 production, water level (WL) serves as an effective on/off switch mechanism, often dictating the presence or absence of CH_4 production (Leppala et al., 2011; Sha et al., 2011; Sturtevant et al., 2012). However, the relationship between the WL and CH_4 flux remains inadequately understood. Prior investigations have suggested that a decline of 1 cm in WL inhibits CH_4 emissions by 1.055 (0.8–1.309) mg m^{-2} h^{-1} in global peatland wetlands (Huang et al., 2021). Nevertheless, within the Yangtze River floodplain, the dominant factor influencing CH_4 emissions has been observed to vary across different stages (i.e., flooding and non-flooding), with the relationship between CH_4 flux and WL displaying variable correlations rather than a fixed positive or negative trend (Gao et al., 2016). In general, anaerobic conditions are imperative for soil CH_4 production. Flooding events that result in high WL in floodplain wetlands create an anaerobic soil environment, promoting CH_4 production and potential pulse-like emissions. Similar phenomena have been recently observed in coastal wetlands and reservoirs (Li et al., 2018, 2022). However, the occurrence of pulse-like phenomenon in floodplain wetlands remains insufficiently confirmed because of the effects of flood inundation, and as a result, the precise magnitude of the stimulating effect of flooding on CH_4 emissions remains unclear.

In addition to WL, soil and/or air temperature exert a strong influence on CH_4 emissions, likely attributable to the stimulation of metabolic rates within the microbial methanogenic flora inhabiting the soil. Higher air temperatures are often associated with increased soil temperature and CH_4 flux (Dengel et al., 2013; Mitsch et al., 2010; Morin et al., 2014; Sachs et al., 2010). Furthermore, temperature and WL frequently undergo simultaneous changes, thereby exerting a combined influence on CH_4 production and emissions within the ecosystem. The intricate nature and variability of these environmental factors pose considerable challenges in accurately estimating CH_4 fluxes and drawing definitive conclusions. Therefore, accurate monitoring of CH_4 fluxes and comprehensive analysis of its environmental effects are of paramount importance, particularly in floodplains characterized by frequent fluctuations in water regime.

This study aimed to examine the variation in CH_4 fluxes and their associated environmental factors throughout a three-year flooding period (2019–2021) within the *M. sacchariflorus* ecosystem of the Dongting Lake floodplain. Two distinct flooding regimes were observed for the respective years: a single flooding event in 2019 and 2020 and multiple flooding events (three occurrences) in 2021. Three hypotheses were formulated: (1) CH_4 emissions would significantly increase during the flooding period because of the anaerobic soil conditions resulting from inundation; (2) For the year with multiple flooding events, CH_4 emission rates would significantly reduce as CH_4 can be oxidized during the flooding intervals; and (3) CH_4 fluxes within the *M. sacchariflorus* ecosystem would exhibit a significant relationship with above-ground WL (i.e., water depth) and temperature.

2. Materials and methods

2.1. Study site

The Dongting Lake (28°30′–30°20′N, 111°40′–113°10′E) is the second largest inland freshwater lake in China, covering an area of approximately 2625 km^2 (Zhu et al., 2022). This lake receives inflow from the Yangtze River through three channels, namely the Songzi, Hudu, and Ouchi rivers, along with four tributaries known as the Xiang, Zi, Yuan, and Li rivers. Subsequently, the lake's water flows back into the Yangtze River at Chenglingji, Hunan Province (Geng et al., 2021). Notably, the lake's wetlands undergo important seasonal fluctuations in water levels, ranging from 12 to 14 m. The maximum WL typically occurs in July or August, whereas the minimum WL is observed in January or February, providing the fundamental hydrological conditions necessary for maintaining extensive floodplain wetlands (Deng et al., 2018). Moving from the water edge to the uplands, the general pattern of plant zonation consists of distinct communities, including the *Phalaris arundinacea* community (referred to as Phalaris hereafter), *Carex brevicuspis* (Carex), *Polygonum hydropiper* (Polygonum; typically interspersed within the Carex zone), and *Miscanthus sacchariflorus* (*M. Miscanthus*) (Chen et al., 2014; Xie and Chen, 2008). The study was conducted in Junshan (29°29′N, 113°03′E), where the dominant vegetation type corresponds to the *M. sacchariflorus* community. The study area experiences a subtropical monsoon climate, characterized by average temperatures ranging from 14.6 °C to 17.5 °C during the period from 2019 to 2021. The lowest temperatures occur in January (3.19–5.93 °C) and the highest temperatures occur in July or August (28.9–29.6 °C). Furthermore, the annual average precipitation in the region amounts to 1200 mm, with 60% of the rainfall occurring between April and August.

2.2. Flux measurements

CH_4 fluxes were measured using an EC system consisting of a 3D sonic anemometer (CSAT-3, Campbell Scientific, USA), positioned at a height of 8.5 m, and an open-path infrared CH_4 gas analyzer (LI-7700, LI-COR, USA). The CH_4 gas analyzer was equipped with an automated pumping system that utilized purified water to cleanse the lower specular surface whenever the signal strength dropped below 20%. The flux tower was situated on flat terrain within a predominantly *M. sacchariflorus* vegetation cover. Two environmental variables, air temperature (T_{air}) and water depth (WD), were measured using a CH_4 gas analyzer and a water-level gauge (HOBO, USA), respectively. Rainfall data were collected from a rain gauge (Texas Electronics, USA). These measurements were conducted from April 2019 to December 2021 at a frequency of 10 Hz and stored on a data logger (CR1000, Campbell Scientific, USA).

2.3. Flux calculation and gap filling

Raw data were acquired using a 10 Hz frequency eddy correlation system and subsequently processed employing the LoggerNet software. Half-hourly fluxes were computed using EddyPro 7.0.6, encompassing various statistical analysis such as spike removal, amplitude resolution, drop-outs, and absolute limits, as well as conducting double coordinate rotation, uncorrected flux calculations, turbulent fluctuations through block averaging, and applying the Weber–Pearman–Leuning (WPL) correction method (Chen et al., 2021a; Jiemin et al., 2007; Mcdermitt et al., 2011). Any abnormal data points, such as −9999, resulting from instrument malfunctions were excluded. The processed data generated by EddyPro 7.0.6 were categorized into three quality grades of 0, 1, and 2. Grade 2 data were removed and only grades 0 and 1 data were retained for further analysis (Foken et al., 2004). Interpolation of the data was not performed as it was intended for correlation analysis with environmental factors. The CH_4 flux for each day was expressed as the average of 48 instantaneous values recorded throughout the day, accounting for any outliers present.

Missing data in CH_4 flux measurements were addressed using an artificial neural network (ANN). This method has recently demonstrated notable efficacy in filling gaps in CH_4 flux data (Dengel et al., 2013; Moffat et al., 2007; Wang et al., 2018). The ANN implementation was performed using the MatLab numerical software. The dataset was divided into daytime and nighttime subsets based on a threshold of 20 μmol m^{-2} s^{-1} for PPFD. To train the network, 70% of the available data in each subset was used, another 15% allocated for testing, and the remaining 15% for validation (Dengel et al., 2013; Moffat et al., 2010). The neural network architecture was initialized 10 times with randomly assigned weight values, and the initialization resulting in the lowest average sampling error was selected (Jarvi et al., 2012). The simplest architecture was chosen, considering that increased complexity did not yield a decrease in mean square error of less than 5%, and the predicted results were saved. Therefore, the number of neurons in the hidden layer of the fitting network was set to 10. This procedure was repeated 20 times and the median predictions were employed to fill the missing half-hourly fluxes (Elizondo and Gongora, 2005). The ANN was trained with the Levenberg–Marquard backpropagation algorithm in MatLab (trainlm) (Dengel et al., 2013). Consistent with previous studies, the selected input variables included air temperature, underground soil temperature, solar radiation, vapor pressure deficit (VPD), u* and relative humidity (RH) (Dengel et al., 2013). Given the substantial difference between flood and non-flood periods, the two periods were treated separately during the gap-filling process. It is important to note that the gap-filled flux data were solely employed for CH_4 budgeting in this analysis.

2.4. *Defining flooding time-lag effects and calculating the effect of flood stimulation on CH_4*

To accurately capture the flood-stimulation effect on CH_4 emissions, data from approximately 25 days prior to the flood were selected for comparison. Flood inundation dates were determined by analyzing the monitored WD data in the *M. sacchariflorus* ecosystem. To determine the date of the mutation point in CH_4 emissions, we employed the Manner–Kendall (MK) trend mutation analysis (Figs. S1, S2, S3). The time-lag effect was calculated by subtracting the date of inundation from the date of the mutation point in CH_4 emissions.

$$T_E = T_{CH_4} - T_{flood} \tag{1}$$

In which, T_E represents time-lag effect, T_{CH_4} represents the date of the mutation point in CH_4 emissions, T_{flood} represents the date of inundation.

Furthermore, the stimulation effect of flooding on CH_4 emissions was quantified as the difference between the average CH_4 flux during the flooding period and the average CH_4 flux prior to the flooding period (Moore and Dalva, 1993).

$$S_E = F_{CH_4-flood} - F_{CH_4-beforeflood} \tag{2}$$

In which, S_E represents the stimulation effect of flooding on CH_4 emissions, $F_{CH_4-flood}$ represents the average CH_4 flux during the flooding period, $F_{CH_4-beforeflood}$ represents the average CH_4 flux prior to the flooding period.

It is important to note that data for the year 2020 were excluded from the time-lag analysis due to the absence of data for approximately one-third of the flood period, resulting from electronic instrument failure and frequent rainfall.

In this study, we explored the relationship between the CH_4 fluxes and two key environmental variables: WD and T_{air}. The time-lag effect in the M. sacchariflorus ecosystem was also considered; however, determining the exact point at which the time-lag effect disappears poses challenges, as it can considerably affect the correlation analysis and complicate the establishment of a clear cause-and-effect relationship (Mitra et al., 2020). To mitigate the influence of the time-lag effect, we focused our analysis on the CH_4 fluxes during the receding stage (the WD continuously decreases to 0 m) in relation to WD and T_{air}, during which the M. sacchariflorus ecosystem remained inundated (Fig. 1).

3. Results

3.1. *Variations in environmental factors and CH_4 fluxes*

The duration of the flooding period varied significantly across different years. Specifically, from 2019 to 2021, the flooding lasted 58, 121, and 87 days, respectively (Fig. 2a). Compared with the highest WD recorded, which reached 3.61 m in 2019 and 2.19 m in 2021, it is noteworthy that the WD peaked at 5.70 m in 2020. Notably, while the *M. sacchariflorus* ecosystem experienced a single flood rise and fall process in 2019 and 2020, it experienced three such processes in 2021 (Fig. 2a). In terms of precipitation, the recorded values for 2019, 2020 and 2021 were 940.3 mm, 1613.5 mm, and 1048.5 mm, respectively, with over 60% of the precipitation occurring between March and July. The high-intensity precipitation observed in 2020 indicated a flood year, characterized by the highest WD and longest flooding duration. Throughout the observation period, the minimum air temperature recorded was −4.8 °C, while the maximum air temperature reached 32.4 °C. On average, the air temperature for 2019, 2020, and 2021 was 17.5 °C (Fig. 2b).

In the *M. sacchariflorus* ecosystem, CH_4 emissions were predominantly observed during the flood period, displaying a range of CH_4 flux values from −0.007 to 0.416 g CH_4—C m^{-2} d^{-1} (with a mean value of 0.043 g CH_4—C m^{-2} d^{-1} across the years 2019, 2020 and 2021). The fluctuation in CH_4 flux over the period from 2019 to 2021 ranged between −0.007–0.416 g CH_4—C m^{-2} d^{-1}, −0.003–0.188 g CH_4—C m^{-2} d^{-1} and −0.005–0.296 g CH_4—C m^{-2} d^{-1}, with corresponding mean values of 0.044 g CH_4—C m^{-2} d^{-1}, 0.053 g CH_4—C m^{-2} d^{-1} and 0.033 g CH_4—C m^{-2} d^{-1}, respectively (Fig. 2a).

3.2. *Interannual variation in CH_4 budget*

CH_4 emissions were found to be low during non-flood periods, with most emissions being concentrated during flood periods. The accumulation of CH_4 exhibited a sharp increase during flood periods, while showing a lower rate of increase during non-flood periods. Notably, the flood period in 2020 persisted for the longest duration, spanning 121 days, resulting in the highest CH_4 accumulation of 19.56 g CH_4—C m^{-2} y^{-1}. Conversely, the CH_4 accumulation in 2019 and 2021 was 12.09 g CH_4—C m^{-2} y^{-1} and 11.97 g CH_4—C m^{-2} y^{-1}, respectively, with a mean value of 14.54 g CH_4—C m^{-2} y^{-1} across the years 2019, 2020 and 2021 (Fig. 3).

3.3. *Variation in CH_4 flux during flood periods*

The CH_4 flux observed during the flood period exhibited positive values, indicating CH_4 emissions, whereas sporadic occurrences of small negative CH_4 flux values suggested either absorption or CH_4 oxidation during the pre-flood period. Under flooding conditions, CH_4 emissions increased sharply, with maximum emissions reaching 0.436 g CH_4—C m^{-2} d^{-1} in 2019, 0.386 g CH_4—C m^{-2} d^{-1} in 2020, and 0.319 g CH_4—C m^{-2} d^{-1} in 2021 (Fig. 4a). Comparatively, these values were significantly higher than the corresponding values in the pre-flood period, measuring 0.188 g CH_4—C m^{-2} d^{-1}, 0.179 g CH_4—C m^{-2} d^{-1}, and 0.097 g CH_4—C m^{-2} d^{-1} in the 2019, 2020, and 2021 flood periods, respectively, and 0.011 g CH_4—C m^{-2} d^{-1}, 0.009 g CH_4—C m^{-2} d^{-1}, and 0.021 g CH_4—C m^{-2} d^{-1} in the 2019, 2020, and 2021 pre-flood periods, respectively. The gradual increase in CH_4 emissions corresponded with the progression of inundation in the initial stage of flooding. The analysis of the MK trend mutation (Figs. S2 and S3) indicated a significant time-lag effect of flood inundation on CH_4 emissions, with a consistent

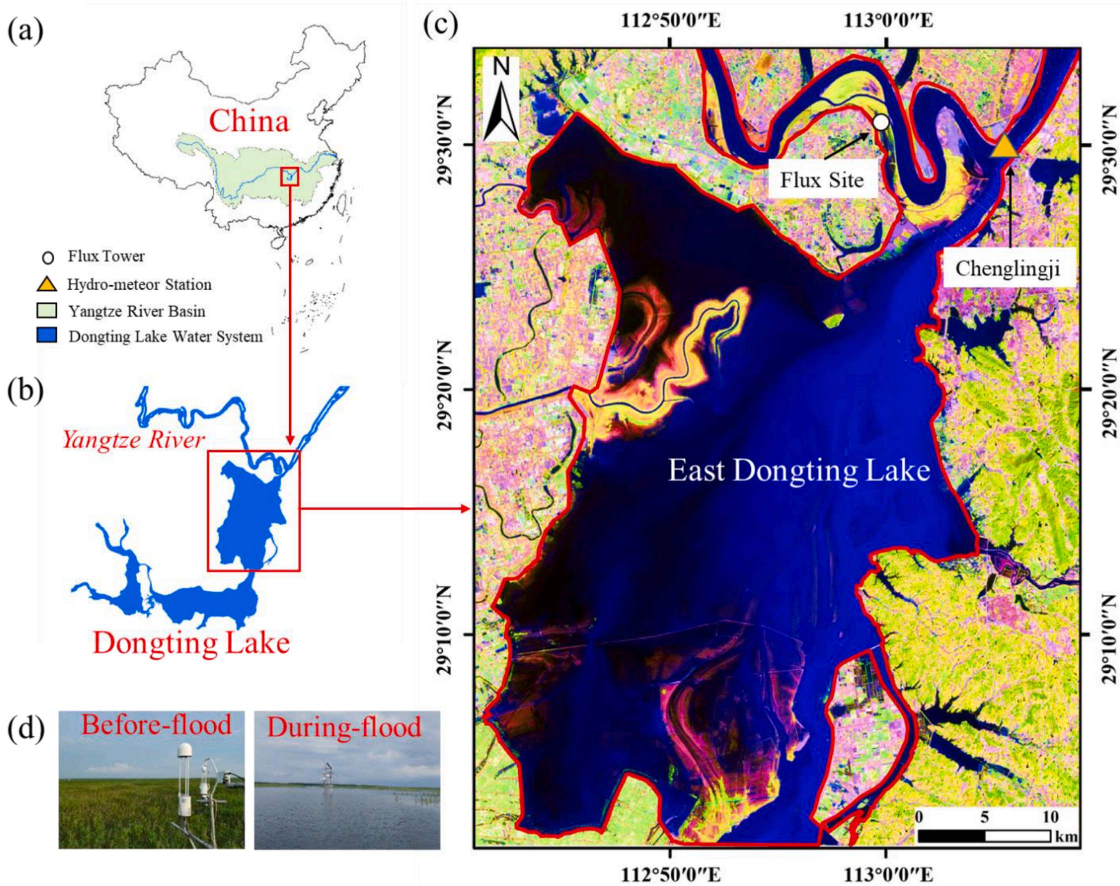

Fig. 1. Map of the study zones in the Dongting Lake wetlands. (a) Location of the Yangtze River basin relative to China; (b) location of Dongting Lake with respect to the Yangtze River Basin; (c) location of the flux tower and hydrometeor station in East Dongting Lake; and (d) physical view of the before-flood and during-flood stages of the *M. saccharifloru*s community.

10-day time-lag effect observed in both 2019 and 2021 (Fig. 4a). These findings suggest that flood events have a discernible impact on CH_4 emissions, and the time-lag effect further underscores the complexity of the relationship between flood inundation and CH_4 dynamics in the studied ecosystem.

The WD data provided insights into the flooding patterns in the *M. saccharifloru*s ecosystem across the study period. In 2019 and 2020, the ecosystem experienced continuous flooding, while three distinct flood fluctuation processes occurred in 2021 (Fig. 2). Each flood event stimulated CH_4 emissions, leading to a considerable increase compared to the pre-flood period. As depicted in Fig. 4b, the flood-induced stimulation of CH_4 emissions in 2019, 2021–1, 2021–2, and 2021–3 (representing the three flood periods in 2021), was 0.177 g CH_4—C m^{-2} d^{-1}, 0.140 g CH_4—C m^{-2} d^{-1}, 0.056 g CH_4—C m^{-2} d^{-1}, and 0.054 g CH_4—C m^{-2} d^{-1}, respectively. We considered the 2019 and 2021–1 events as first-floods (FFs) and 2021–2 and 2021–3 as repeat-floods (RFs). Notably, the stimulation effect of flooding on CH_4 emissions was significantly reduced during RFs (0.055 g CH_4—C m^{-2} d^{-1}) compared to FFs (0.159 g CH_4—C m^{-2} d^{-1}) (Fig. 4c). Overall, the continuous flooding year demonstrated a greater stimulation effect on CH_4 emissions than the RF year. Consequently, our findings suggest that intermittent flooding is preferable to continuous flooding to mitigate CH_4 emissions (Fig. 4).

3.4. Controls on CH_4 emissions during flooding

The Gaussian 2-D regression model successfully simulated the relationship among the CH_4 flux, WD, and T_{air} in the *M. saccharifloru*s ecosystem ($R^2 = 0.554$, $P < 0.05$) (Table 1). Contour plots depicting CH_4 flux in the *M. saccharifloru*s ecosystem revealed a continuous increase in CH_4 emissions with decreasing WD and increasing T_{air} (Fig. 5).

4. Discussion

4.1. Annual budget and interannual variation in CH_4 emissions

From 2019 to 2021, CH_4 emissions mainly occurred during flood periods, with the highest CH_4 emissions in 2020 (19.56 g CH_4—C m^{-2} y^{-1}) and comparatively lower emissions in 2019 (12.09 g CH_4—C m^{-2} y^{-1}) and 2021 (11.97 g CH_4—C m^{-2} y^{-1}). Compared to various wetland ecosystems worldwide, CH_4 emissions observed within the *M. saccharifloru*s community in the Dongting Lake floodplain were relatively higher than those documented in tidal wetlands, peatlands, and other floodplains (Fig. 4; Table 2). For instance, the wetland floodplain of the Northern Pantanal, where the dominant species is Combretum lanceolatum (Dalmagro et al., 2019), has hydrological characteristics similar to those of the Dongting Lake. Nevertheless, the CH_4 emissions during the flooding period (0.113 g CH_4—C m^{-2} d^{-1}) were considerably lower than those in the Dongting Lake (0.155 g CH_4—C m^{-2} d^{-1}). One possible explanation for this discrepancy is that the dominant species in the Dongting Lake, M. sacchariflorus, possesses well-developed aeration tissue that may promote CH_4 emissions (Brix et al., 1992). Tidal wetlands, particularly brackish marshes, emit considerably lower quantities of CH_4 compared to freshwater marshes due to the constraints imposed by high salinity (Holm et al., 2016). Furthermore, the CH_4 emissions recorded in the Dongting Lake floodplain wetlands surpass those in peatland wetlands (Chen et al., 2021a; Tang et al., 2018) and are an order of magnitude higher than those in

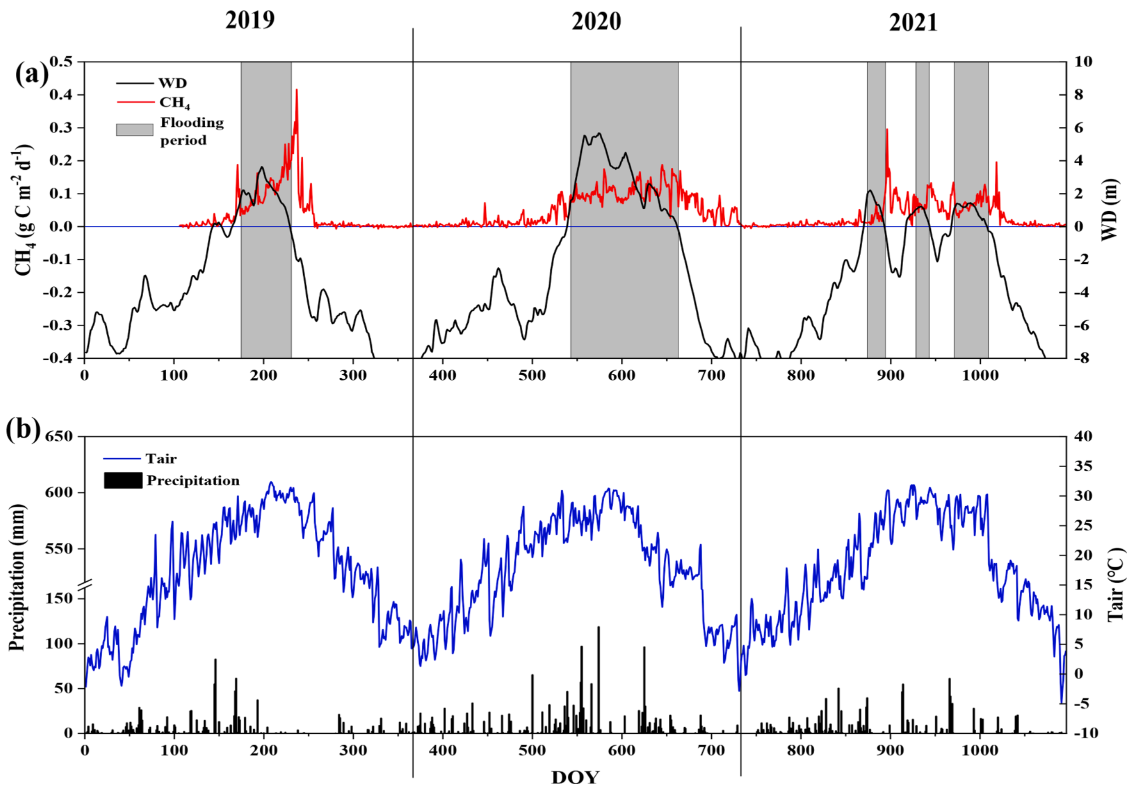

Fig. 2. (a) Interannual variation in CH_4 flux of the *M. saccharifloru*s ecosystem, WD > 0 means flooding, with gray shaded areas indicate flooding periods, (b) air temperature (T_{air}) and total daily precipitation in the floodplain wetlands of Dongting Lake from 2019 to 2021.

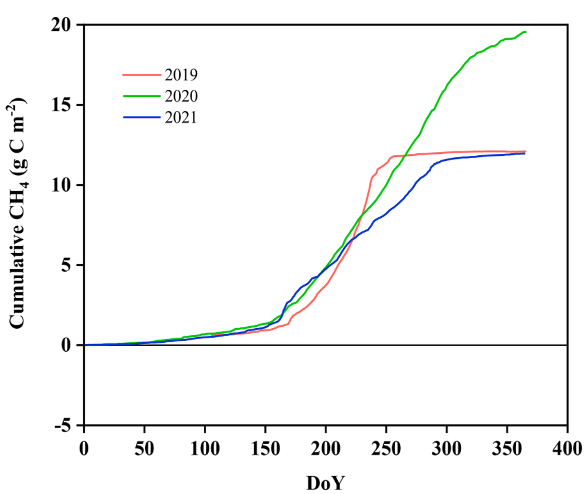

Fig. 3. Cumulative annual CH_4 for the *M. saccharifloru*s ecosystem 2019–2021. Due to frequent rainfall and instrument malfunctions in 2020, there were too many missing data and the data quality declined, which may lead to overestimation of CH_4 emissions during data interpolation.

coastal wetlands (Li et al., 2018) (Table 2).

The interannual variations in our study site suggest a potential influence of hydrological rhythms, such as flood duration and frequency, on CH_4 emissions. On one hand, the longest flood duration in 2020 contributed to the highest CH_4 emissions. On the other hand, frequent rainfall and instrument malfunctions in 2020 resulted in compromised data quality and missing data, potentially leading to an overestimation of CH_4 emissions during data interpolation. Despite the increased number of flood days in 2021 compared to 2019, there was no significant difference in CH_4 emissions between these two years. This lack of difference could be attributed to the high flood frequency in 2021, which may have contributed to decreased CH_4 emissions (Fig. 4c).

4.2. Flood-stimulation effects on CH_4 emissions

Our results demonstrated that the average CH_4 emissions during the flooding season within the *M. saccharifloru*s ecosystem amounted to 0.155 g CH_4—C m^{-2} d^{-1}, a substantially higher value compared to the pre-flood period emissions of approximately 0.014 g CH_4—C m^{-2} d^{-1} (Fig. 4). These findings provide robust confirmation of our first hypothesis, highlighting a substantial increase in CH_4 emissions during the flooding period. The WD plays a critical role in regulating CH_4 production, resembling an on-or-off switch that either triggers or inhibits the process (Mitra et al., 2020; Morin et al., 2014). In the Dongting Lake floodplain, the onset of floods triggers the transformation of the M. saccharifloru*s* ecosystem into an anaerobic environment, leading to a sharp rise in the soil methanogenic potential and, consequently, leading to higher CH_4 emissions (Huai et al., 2006; Wang et al., 2018b). This phenomenon may be regarded as the primary driving force behind the observed stimulation effect on CH_4 emissions.

4.3. Effects of the flooding regime on CH_4 emissions

Our study revealed distinct CH_4 emission rates during the flood period, with values of 0.188 ± 0.016, 0.179 ± 0.009, and 0.097 ± 0.007 g CH_4—C m^{-2} d^{-1} in 2019, 2020, and 2021, respectively (Fig. 4a). There was no significant difference in CH_4 emission rates between the 2019 and 2020 flood periods; however, both years exhibited significantly higher rates than the 2021 flood period (Fig. 6). These findings highlight the influence of different flooding regimes on CH_4 emission rates, including the rate, frequency, duration, and inundation depth of floods in different years. Notably, in 2019 and 2020, the *M. saccharifloru*s ecosystem experienced continuous flooding and a single flood rise–fall process. Whereas in 2021, multiple flooding occurred with three flood rise–fall processes (Fig. 2; Fig. S1). There was a

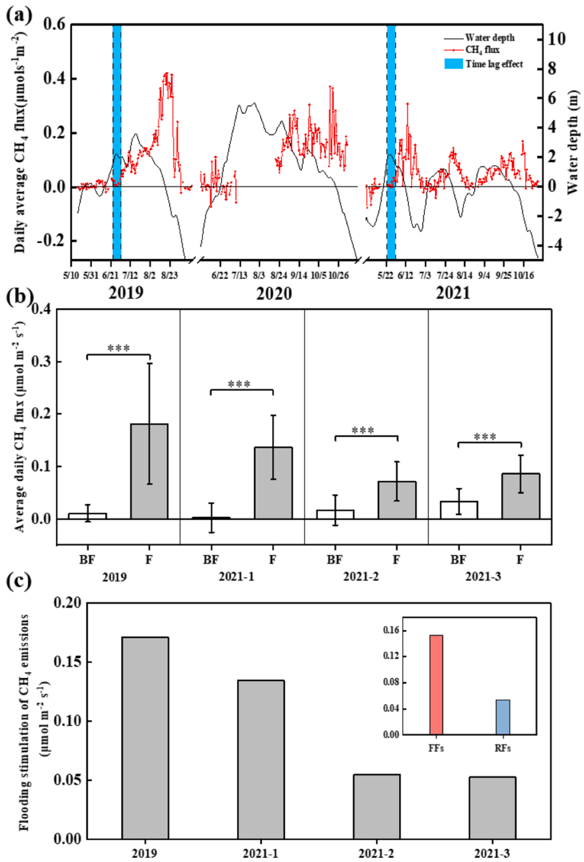

Fig. 4. (a)Variation in the *M. sacchariflorus* ecosystem daily average CH_4 flux during the flood period and the time lag effect of CH_4 emissions. (b)Effect of flood stimulation and (c)repeated inundation on CH_4 emissions. BF = before-flood (approximately 25 days prior to the flood); F = flood; FFs = first-flood stages; RFs = repeated-flood stages. During the observation period, data were lost owing to weather and instrument failure. Significant changes are marked with an asterisk ($p < 0.05$).

Table 1
Regression models of WD and T_{air} on the control of CH_4 fluxes in the *M. sacchariflorus* ecosystem during floods ($n = 74$).

Dependent variables	Regression model	R^2	F	P
CH_4 flux	$F_{CH4} = 2.413 + 0.313{*}WD{-}0.198{*}T_{air} + 0.053{*}WD^2 + 0.004{*}T_{air}^2{-}0.018{*}WD{*}T_{air}$;	0.554	19.148	<0.05

similarity pattern in the flood-stimulation effect on CH_4 emissions between the 2021–1 and 2019 phases; however, the stimulation effect was reduced by more than half in the 2021–2 and 2021–3 phases, indicating that increased flooding frequency mitigates the stimulation effect on CH_4 emissions (Fig. 4c). These results confirmed our second hypothesis, suggesting that multiple flooding events can effectively reduce the rate of CH_4 emissions compared to continuous flooding. The frequent alternation between aerobic and anaerobic environments poses challenges for the survival of methanogenic bacteria; however, an anaerobic environment provides favorable conditions for their activity, leading to high CH_4 emission rates (Datta et al., 2013; Singh, 2011). This regulatory model provides scientific guidance for managing CH_4 emissions in floodplain wetlands by regulating WD changes through sluices to modulate the frequency of flooding, thereby mitigating CH_4 emissions.

4.4. Time-lag effect of flooding on CH_4 emissions

The MK trend mutation analysis revealed a time-lag effect of flooding on CH_4 emissions of approximately 10 days in the Dongting Lake M. sacchariflorus ecosystem (Fig. 4). This phenomenon has also been reported in various studies. For instance, Li et al. (2019) conducted a study using a wavelet coherence analysis in a rice paddy ecosystem and found a time-lag effect of 3–7 h. Controlled laboratory experiments employing stable isotope labeling in rice revealed a strong immediate relationship between photosynthesis and CH_4 flux, with a time-lag of 2–3 days between CO_2 assimilation and CH_4 emission (Dannenberg and Conrad, 1999; Minoda et al., 1996). Moore and Dalva (1993) observed a lag period of up to 10 days between the rise of groundwater levels in the peat column surface and the onset of significant CH_4 emissions. The relationship between variations in the environmental variables and microbial responses in CH_4 production and consumption may explain these time-lag effect (Moore and Dalva, 1993). It is important to note that although flooding creates an anaerobic environment, the onset of CH_4 emissions does not occur immediately upon inundation. Additionally, variations in factors such as soil compactness, vegetation type, organic carbon content, and surrounding environmental conditions (temperature, radiation, pressure, etc.) can contribute to different time-lag effects on CH_4 emissions. Further research is necessary to delve into these findings and deepen our understanding of these complex dynamics in future studies.

4.5. Relationship between WD, T_{air} and CH_4 emissions

The results obtained from the data collected over a span of two years (2019 and 2021) revealed a continuous increase in CH_4 emissions with decreasing WD and increasing T_{air}, which supported our third hypothesis (Table. 1; Fig. 5). It is important to analyze the relationship between CH_4 flux and WL in two scenarios: above-ground WL (i.e., WD) and below-ground WL. Several studies have consistently reported a positive correlation between CH_4 emissions and below-ground WL, wherein higher below-ground WL values contribute to increased CH_4 emissions (Chen et al., 2021b; Fortuniak et al., 2021; Huang et al., 2021; Moore and Roulet, 1993). However, research conducted on lake wetlands has demonstrated a linear decrease in CH_4 diffusion flux with rising WD (Li et al., 2020; Xiao et al., 2017), which is consistent with the observed trend in our study. Similar patterns have also been observed in peat wetlands (Chen et al., 2021a). The negative relationship between WD and CH_4 flux can be explained by the following three approaches: 1) Within the Dongting Lake region, the M. sacchariflorus community reaches approximately 4 m in height and has well-developed rhizome and aeration tissues. An inverse relationship has been observed between plant-mediated CH_4 emissions and WD as well as the submerged fraction of stems and leaves (Gauci et al., 2010; Pangala et al., 2013; Pitz et al., 2018). Consequently, higher WD values and greater submergence of plant biomass correspond to lower plant-mediated CH_4 emissions. 2) Elevated WD exert increased hydrostatic pressure on the M. sacchariflorus ecosystem, which inhibited the CH_4 bubble release from the lake bottom, and thus limiting the release of CH_4 emissions (Iwata et al., 2020). 3) A comparison of oxic to anoxic soils in wetlands reveal up to ten times greater CH_4 production and nine times more methanogenesis activity in oxygenated soils (Angle et al., 2017). Thus, during floods, a shallow WD fosters higher water and soil oxygen levels, potentially resulting in increased CH_4 emissions.

The analysis of our data revealed an increase in CH_4 emissions with increasing T_{air}. This outcome may be attributed to the broader range of T_{air} variation encompassed by the two-year dataset (24.3–32.4 °C), which revealed a discernible pattern between CH_4 emissions and T_{air}. Furthermore, the optimal temperature for CH_4 production varied across different soil types; Svensson (1984) proposed optimal temperatures of 20 °C and 28 °C for methanogenic bacteria using acetic acid and H_2, respectively. Experiments conducted in Finnish marshes reported high

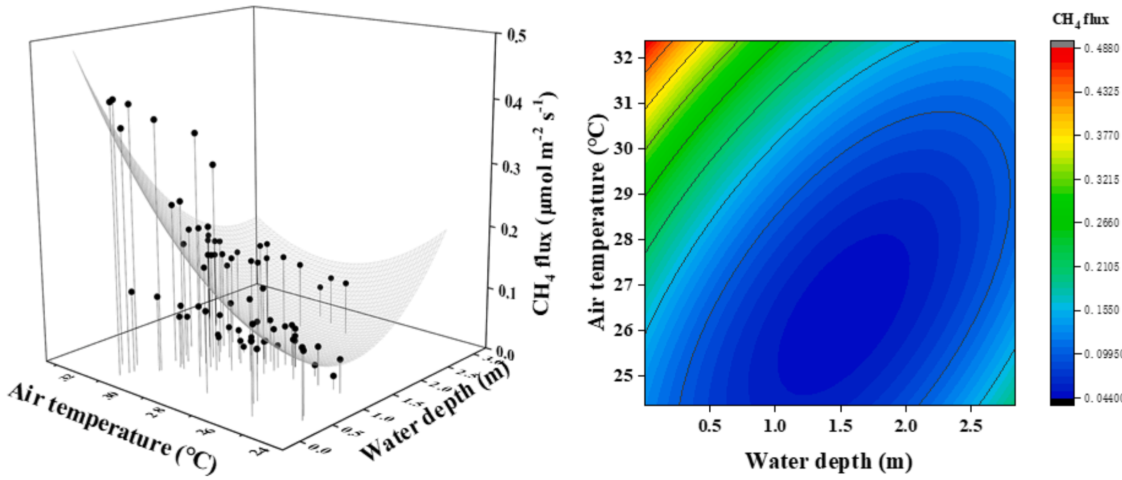

Fig. 5. Response of the CH_4 flux to the water depth (WD) and air temperature (T_{air}) in the *M. sacchariflorus* ecosystem during flood recession. The responses of the 2019 and 2021 CH_4 fluxes to WD and T_{air} in the *M. sacchariflorus* ecosystem were fitted using Gaussian 2-D nonlinear surface fitting methods and kriging gridding methods (2019: $n = 35$; 2021: $n = 39$).

Table 2
Comparison of the net ecosystem CH_4 exchange (NEE-CH_4) in different wetland ecosystems worldwide.

Reference	Wetland Type	Location	Dominant vegetation	Average daily NEE (g CH_4–C m^{-2} d^{-1})	Study period
This study	Floodplain	Dongting lake (China) (29°29′ N, 113°03′ E)	*Miscanthus sacchariflorus*	0.155	07.2019–08.2019 07.2020–10.2020 06.2021–09.2021
(Dalmagro et al., 2019)	Floodplain	Northern Pantanal (Brazil) (16°29′ S, 56°24′ W)	*Combretum lanceolatum*	0.113	01.2014–06.2014 01.2015–06.2015 02.2016–06.2016 11.2016–06.2017
(Chen et al., 2021)	Peatland	Zoige (China) (33°06′ N, 102°39′ E)	*Carex muliensis, Trollius farreri Stapf*	0.103	01.2013–12.2014 01.2016–12.2017
(Holm et al., 2016)	Tidal (Freshwater marsh) (Brackish marsh)	Louisiana (United States) (29°51′ N, 90°17′ W) (29°30′ N, 90°26′ W)	 *Sagittaria lancifolia, Leersia ory-zoides*, and *Typha domingensis* *Spartina patens; Schoenoplectus americanus*	 0.128 0.029	 12.2011–12.2013 10.2011–12.2012
(Tang et al., 2018)	Peatland	Betong division (Malaysia) (1°27′ N, 111°9′ E)	*Shorea albida, Gonystylus banca-nus*, and *Stemonurus spp*	0.024	11.2013–12.2013
(Li et al., 2018)	Coastal	Chongming island (China) (31°31′ N, 121°57′ E)	*Phragmites australis* and *Spartina alterniflora*	0.048	04.2011–11.2012

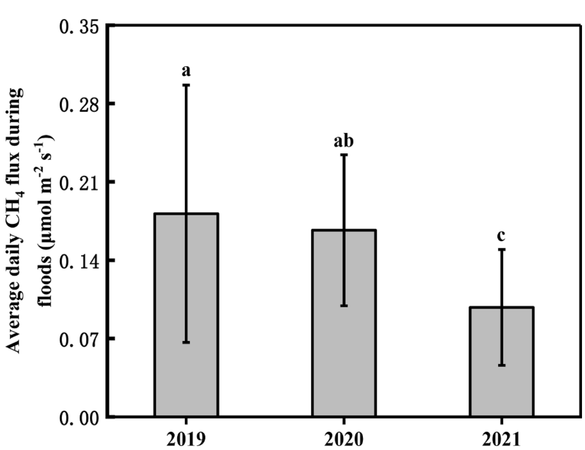

Fig. 6. Mean CH_4 fluxes during floods in different hydrological years. Different letters indicate significant differences among the treatments at the 0.05 significance level.

CH_4 production at 4 °C, while a diminished temperature-response effect on CH_4 production was observed at temperatures exceeding 20 °C (Ding and Cai, 2003; Frenzel and Karofeld, 2000). Considering the relatively higher sensitivity of T_{air} compared to subaqueous soil temperature, which was closely related to CH_4 emissions, it is crucial to refine our understanding of the relationship between T_{air} fluctuations and CH_4 emissions during floods through long-term investigations encompassing large volumes of data.

5. Conclusions

In this study, we conducted measurements of CH_4 fluxes in the floodplain wetlands of the Dongting Lake. The cumulative interannual emissions of CH_4 indicated that the floodplain wetlands of Lake Dongting were an important natural source of CH_4. The increased frequency of inundation reduced the rate of CH_4 emissions from these wetlands. Furthermore, WD changes and T_{air} appear to be the key environmental factors for controlling CH_4 emissions throughout the flood period. Specifically, reducing the WD and increasing the T_{air} under flooded conditions was observed to substantially enhance CH_4 release. It should be noted that this study is limited by focusing solely on *M. sacchariflorus*, as the Dongting Lake area comprises various wetland plant species, each contributing with different CH_4 emissions. Therefore, more observation should be carried out on different vegetation types in the future to enable more accurate estimations of CH_4 emissions from Dongting Lake floodplain. Overall, given the ongoing global change trend, ensuring the optimization of hydrological conditions in floodplain wetlands may be critical for mitigating CH_4 emissions from flooded wetlands.

Declaration of Competing Interest

This manuscript has not been published or presented elsewhere in part or in entirety and is not under consideration by another journal. We have read and understood your journal's policies, and we believe that neither the manuscript nor the study violates any of these. There are no conflicts of interest to declare.

Data availability

The authors do not have permission to share data.

Acknowledgments

This research was supported by the National Natural Science Foundation of China (32071576), Joint Fund for Regional Innovation and Development of NSFC (U22A20570, U21A2009), National Key Research and Development Program (2022YFC3204101), Hunan Natural Science Fund for Distinguished Young Scholars (2022JJ10055), the Key Program of Science and Technology of the Ministry of Water Resources (SKS-2022081), Youth Promotion Association of the Chinese Academy of Sciences, Changsha Natural Science Funds for Distinguished Young Scholars (2021), and Hunan Key Laboratory of Remote Sensing Monitoring of Ecological Environment in Dongting Lake area (DTH key Lab. 2021-027), Comprehensive Investigation and Potential Evaluation of Natural Resources Carbon Sink in Southern Hilly Region (ZD20220136). We would like to thank Editage (https://www.editage.cn/) for the English language editing of an earlier version of the manuscript.

Supplementary materials

Supplementary material associated with this article can be found, in the online version, at doi:10.1016/j.agrformet.2023.109677.

References

Anderson, D., Verma, S., Rosenberg, N., 1984. Eddy correlation measurements of CO_2, latent heat, and sensible heat fluxes over a crop surface. Bound. Layer Meteorol. 29 (3), 263–272.
Angle, J.C., et al., 2017. Methanogenesis in oxygenated soils is a substantial fraction of wetland methane emissions. Nat. Commun. 8 (1), 1567.
Batson, J., et al., 2015. Soil greenhouse gas emissions and carbon budgeting in a short-hydroperiod floodplain wetland. J. Geophys. Res. Biogeosci. 120 (1), 77–95.
Brix, H., Sorrell, B.K., Orr, P.T., 1992. Internal pressurization and convective gas flow in some emergent freshwater macrophytes. Limnol. Oceanogr. 37 (7), 1420–1433.
Chen, H., et al., 2021a. Methane emissions during different freezing-thawing periods from a fen on the Qinghai-Tibetan plateau: four years of measurements. Agric. For. Meteorol. 297, 108279.
Chen, H., Xu, X., Fang, C., Li, B., Nie, M., 2021b. Differences in the temperature dependence of wetland CO_2 and CH_4 emissions vary with water table depth. Nat. Clim. Change 11 (9), 766–771.
Chen, X.S., et al., 2014. Combined influence of hydrological gradient and edaphic factors on the distribution of macrophyte communities in Dongting lake wetlands, China. Wetl. Ecol. Manag. 23 (3), 481–490.
Dalmagro, H.J., et al., 2019. Radiative forcing of methane fluxes offsets net carbon dioxide uptake for a tropical flooded forest. Glob. Chang Biol. 25 (6), 1967–1981.
Dannenberg, S., Conrad, R., 1999. Effect of rice plants on methane production and rhizospheric metabolism in paddy soil. Biogeochemistry 45 (1), 53–71.
Datta, A., et al., 2013. Seasonal variation of methane flux from coastal saline rice field with the application of different organic manures. Atmos. Environ. 66, 114–122.
Delwiche, K.B., et al., 2021. FLUXNET-CH_4: a global, multi-ecosystem dataset and analysis of methane seasonality from freshwater wetlands. Earth Syst. Sci. Data 13 (7), 3607–3689.
Deng, Z.M., et al., 2018. Hydrologic and edaphic controls on soil carbon emission in Dongting lake floodplain, China. J. Geophys. Res. Biogeosci. 123 (9), 3088–3097.
Dengel, S., et al., 2013. Testing the applicability of neural networks as a gap-filling method using CH_4 flux data from high latitude wetlands. Biogeosciences 10 (12), 8185–8200.
Desjardins, R.L., 1974. Technique to measure CO_2 exchange under field conditions. Int. J. Biometeorol. 18 (1), 76–83.
Ding, W., Cai, Z., 2003. Effect of temperature on methane production and oxidation in soils. J. Appl. Ecol. 14 (4), 604–608.
Elizondo, D.A., Gongora, M.A., 2005. Current trends on knowledge extraction and neural networks. In: Duch, W., Kacprzyk, J., Oja, E., Zadrozny, S. (Eds.), Artificial Neural Networks: Formal Models and their Applications - ICANN 2005, Lecture Notes in Computer Science, pp. 485–490. Pt 2, Proceedings.
Foken, T., et al., 2004. Post-field data quality control. In: Handbook of Micrometeorology: A Guide for Surface Flux Measurement and Analysis, 29. Springer, pp. 181–208.
Fortuniak, K., Pawlak, W., Siedlecki, M., Chambers, S., Bednorz, L., 2021. Temperate mire fluctuations from carbon sink to carbon source following changes in water table. Sci. Total Environ. 756, 144071.
Frenzel, P., Karofeld, E., 2000. CH_4 emission from a hollow-ridge complex in a raised bog: the role of CH_4 production and oxidation. Biogeochemistry 51 (1), 91–112.
Gao, S., et al., 2016. Dynamics and regulation of CH_4 flux in a poplar plantation on a floodplain. Acta Ecol. Sin. 36, 5912–5921.
Gauci, V., Gowing, D.J.G., Hornibrook, E.R.C., Davis, J.M., Dise, N.B., 2010. Woody stem methane emission in mature wetland alder trees. Atmos. Environ. 44 (17), 2157–2160.
Geng, M.M., et al., 2021. Evaluation and variation trends analysis of water quality in response to water regime changes in a typical river-connected lake (Dongting Lake), China. Environ. Pollut. 268 (Pt A), 115761.
Holm Jr, G.O., et al., 2016. Ecosystem level methane fluxes from tidal freshwater and brackish marshes of the Mississippi river delta: implications for coastal wetland carbon projects. Wetlands 36 (3), 401–413.
Huai, C., et al., 2006. Advance in studies on production, oxidation and emission flux of methane from wetlands. Chin. J. Appl. Environ. Biol. 12 (5), 726–733.
Huang, Y., et al., 2021. Tradeoff of CO_2 and CH_4 emissions from global peatlands under water-table drawdown. Nat. Clim. Change 11 (7), 618–622.
Iwata, H., et al., 2020. Temporal and spatial variations in methane emissions from the littoral zone of a shallow mid-latitude lake with steady methane bubble emission areas. Agric. For. Meteorol. 295, 108184.
Jarvi, L., et al., 2012. Seasonal and annual variation of carbon dioxide surface fluxes in Helsinki, Finland, in 2006–2010. Atmosp. Chem. Phys. 12 (18), 8475–8489.
Jiemin, W., Wang, W., Ao, Y., Fanglin, S.U.N., Shuguo, W., 2007. Turbulence flux measurements under complicated conditions. Adv. Earth Sci. 22 (8), 791–797.
Kim, Y., et al., 2020. Gap-filling approaches for eddy covariance methane fluxes: a comparison of three machine learning algorithms and a traditional method with principal component analysis. Glob. Change Biol. 26 (3), 1499–1518.
Kirschke, S., et al., 2013. Three decades of global methane sources and sinks. Nat. Geosci. 6 (10), 813–823.
Leppala, M., Oksanen, J., Tuittila, E.S., 2011. Methane flux dynamics during mire succession. Oecologia 165 (2), 489–499.
Li, H., et al., 2018. Multi-scale temporal variation of methane flux and its controls in a subtropical tidal salt marsh in eastern China. Biogeochemistry 137 (1–2), 163–179.
Li, H., et al., 2019. Does direct-seeded rice decrease ecosystem-scale methane emissions? — A case study from a rice paddy in southeast China. Agric. For. Meteorol. 272-273, 118–127.
Li, M., et al., 2020. The significant contribution of lake depth in regulating global lake diffusive methane emissions. Water Res. 172, 115465.
Li, Y., et al., 2022. Changes in water chemistry associated with rainstorm events increase carbon emissions from the inflowing river mouth of a major drinking water reservoir. Environ. Sci. Technol. 56 (22), 16494–16505.
Mcdermitt, D., et al., 2011. A new low-power, open-path instrument for measuring methane flux by eddy covariance. Appl. Phys. B-Lasers Opt. 102 (2), 391–405.
Minoda, T., Kimura, M., Wada, E., 1996. Photosynthates as dominant source of CH_4 and CO_2 in soil water and CH_4 emitted to the atmosphere from paddy fields. J. Geophys. Res.: Atmos. 101 (D15), 21091–21097.
Mitra, B., et al., 2020. Spectral evidence for substrate availability rather than environmental control of methane emissions from a coastal forested wetland. Agric. For. Meteorol. 291, 9.
Mitsch, W.J., et al., 2010. Tropical wetlands: seasonal hydrologic pulsing, carbon sequestration, and methane emissions. Wetl. Ecol. Manag. 18 (5), 573–586.
Moffat, A.M., Beckstein, C., Churkina, G., Mund, M., Heimann, M., 2010. Characterization of ecosystem responses to climatic controls using artificial neural networks. Glob. Chang. Biol. 16 (10), 2737–2749.
Moffat, A.M., et al., 2007. Comprehensive comparison of gap-filling techniques for eddy covariance net carbon fluxes. Agric. For. Meteorol. 147 (3–4), 209–232.
Moore, T.R., Roulet, N.T., 1993. Methane flux: water table relations in northern wetlands. Geophys. Res. Lett. 20 (7), 587–590.
Morin, T.H., et al., 2014. Environmental drivers of methane fluxes from an urban temperate wetland park. J. Geophys. Res. Biogeosci. 119 (11), 2188–2208.
Pangala, S.R., Moore, S., Hornibrook, E.R.C., Gauci, V., 2013. Trees are major conduits for methane egress from tropical forested wetlands. New Phytol. 197 (2), 524–531.
Pitz, S.L., Megonigal, J.P., Chang, C.H., Szlavecz, K., 2018. Methane fluxes from tree stems and soils along a habitat gradient. Biogeochemistry 137 (3), 307–320.
Ren, Y., et al., 2020. Changes in methane emission and community composition of methane-cycling microorganisms along an elevation gradient in the Dongting lake floodplain, China. Atmosphere 11 (9), 997.

Rosentreter, J.A., et al., 2021. Half of global methane emissions come from highly variable aquatic ecosystem sources. Nat. Geosci. 14 (4), 225–230.
Sachs, T., Giebels, M., Boike, J., Kutzbach, L., 2010. Environmental controls on CH_4 emission from polygonal tundra on the microsite scale in the Lena river delta, Siberia. Glob. Change Biol. 16 (11), 3096–3110.
Saunois, M., et al., 2016. The global methane budget 2000–2012. Earth Syst. Sci. Data 8 (2), 697–751.
Scheller, J.H., Mastepanov, M., Christiansen, H.H., Christensen, T.R., 2021. Methane in Zackenberg valley, NE Greenland: multidecadal growing season fluxes of a high-Arctic tundra. Biogeosciences 18 (23), 6093–6114.
Sha, C., et al., 2011. Methane emissions from freshwater riverine wetlands. Ecol. Eng. 37 (1), 16–24.
Singh, J.S., 2011. Methanotrophs: the potential biological sink to mitigate the global methane load. Curr. Sci. 100 (1), 29–30.
Sturtevant, C.S., Oechel, W.C., Zona, D., Kim, Y., Emerson, C.E., 2012. Soil moisture control over autumn season methane flux, Arctic coastal plain of Alaska. Biogeosciences 9 (4), 1423–1440.
Svensson, B.H., 1984. Different temperature optima for methane formation when enrichments from acid peat are supplemented with acetate or hydrogen. Appl. Environ. Microbiol. 48 (2), 389–394.
Tang, A.C.I., et al., 2018. Eddy covariance measurements of methane flux at a tropical peat forest in Sarawak, Malaysian Borneo. Geophys. Res. Lett. 45 (9), 4390–4399.
Turetsky, M.R., et al., 2014. A synthesis of methane emissions from 71 northern, temperate, and subtropical wetlands. Glob. Chang Biol. 20 (7), 2183–2197.
Verma, S.B., et al., 1992. Eddy correlation measurements of methane flux in a northern peatland ecosystem. Bound. Layer Meteorol. 58 (3), 289–304.
Wang, M., et al., 2018a. Temporal shifts in controls over methane emissions from a boreal bog. Agric. For. Meteorol. 262, 120–134.
Wang, W., et al., 2018b. Soil methane production, anaerobic and aerobic oxidation in porewater of wetland soils of the Minjiang river estuarine, China. Wetlands 38 (3), 627–640.
Winton, R.S., Flanagan, N., Richardson, C.J., 2017. Neotropical peatland methane emissions along a vegetation and biogeochemical gradient. PLoS One 12 (10), e0187019.
Xiao, Q., et al., 2017. Spatial variations of methane emission in a large shallow eutrophic lake in subtropical climate. J. Geophys. Res.: Biogeosci. 122 (7), 1597–1614.
Xie, Chen, X.S., 2008. Effects of three-gorge project on succession of wetland vegetation in Dongting lake. Res. Agric. Mod. 29 (6), 684–687.
Zhang, H., et al., 2019. Annual methane emissions from degraded alpine wetlands in the eastern Tibetan plateau. Sci. Total Environ. 657, 1323–1333.
Zhu, L.L., et al., 2022. Effects of hydrological environment on litter carbon input into the surface soil organic carbon pool in the Dongting lake floodplain. Catena 208, 105761.